
CHAPTER - IV

MAGNETIC PROPERTIES

SECTION - A

HYSTERESIS BEHAVIOUR

4. Introduction

Magnetization is one of the most fundamental properties of ferrites. Spontaneous Magnetization occurs even in the absence of external field and it is most striking property of ferromagnetic materials. The saturation magnetization, coercivity and remanance are studied with the help of hysteresis. The magnetic parameters related to hysteresis help to decide the nature of applications of ferrites. The value of saturation magnetization depends on the nature of cations and their distribution. The ferromagnetic materials contain domains and exhibit the phenomenon of saturation and hysteresis.

The hysteresis properties of ferrites are highly sensitive to their chemical composition, porosity, grain size, crystal structure, cation distribution and microstructure [1]. These properties are also influenced by condition of sintering. On the basis of coercive field (H_c), ferrites have been classified into two categories -

I) Soft ferrites

Ferrites with low H_c are called as "soft ferrites". These are easy to magnetize and demagnetize,

such ferrite have high electrical resistivity and low eddy current losses as reviewed by Lee and Lynch [2]. They are used in the manufacture of transformer cores, motors and generators. High frequency inductance and small hysteresis losses are essential requirement [3]. These are also used in microwave devices.

II) Hard ferrites

Ferrites with high value H_c are called hard ferrites and are used as permanent magnet materials for which high remanance is desirable [4]. They are used in loud speakers, telephones, electrical motors, memory devices in computers etc.

According to Neel [5] the coercive force is related with saturation magnetization, internal stresses, porosity [6] and anisotropy [7]. Snoek, Gorter and Goodenough [8,9,10] showed that in order to obtain large range of saturation magnetization a variety of substitutional ferrites can be prepared. To prepare ferrite with desired device properties, it is necessary to know the magnetic as well as electrical characteristics of ferrite.

4.A.1 Magnetization in Ferrites

The most fundamental property of ferrites is the magnetization. The magnetization result from the

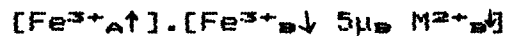
distribution and alignment of magnetic ions on the octahedral and tetrahedral sites. If magnetic atoms are sufficiently close to each other, the spontaneous magnetization (M_s) occurs even in the absence of external field. The electron can undergo an exchange interaction between neighbouring magnetic atoms or ions. This may be direct or may take place via an interatomic interaction. It may be either positive or negative and it is based on parallel and antiparallel alignment of the spins of neighbouring atoms respectively. When the exchange interaction is positive it is ferromagnetic and the alignment is parallel and when it is negative then it is either antiferromagnetic or ferrimagnetic depending upon complete or incomplete cancellation of magnetic moments within the crystals. Gorter arrived at a scheme of spin ordering on the basis of Anderson's concept of superexchange coupling to arrive at a reasonably good value of saturation magnetization.

The saturation magnetization in ferrites is determined by its physico-chemical constitution and also by the cation distribution and other attendant aspects of thermo-physical history. In case of ferrite the solid solubility affords to prepare mixed ferrites, crystallizing in the spinel structure either of normal or of the inverse type. The normal spinels

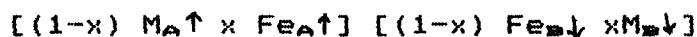
are generally nonmagnetic while inverse spinels are ferrimagnetic. For the ferrite with inverse spinel structure, cation distribution is expressed as



The Fe^{3+} ions on A site are coupled with their spin antiparallel to those Fe^{3+} ions on B-site, so that, net moment is due to divalent M^{2+} metallic ions.



Suppose that M is transition element with n electrons in d-shell. The magnetic moment μ_B per formula unit is $n\mu_B$ or $(10-n)\mu_B$ depending on d-shell which is filled less than half or more than half respectively. The degree of inversion is a fraction 'X' of the divalent metal ions that are on B-site. The arrangement of moment could be written as,



and net magnetic moment is given by difference between moments on A-site and B-site.

$$\mu_B = M [(1-x)] - 10 [1-x]$$

for normal spinel $x = 0$

and for inverse spinel $x = 1$

The indirect exchange coupling between metallic ions acting through the angle AOB is close to 180° . For perfect spinel lattice the major angles between the ions are ABO ($125^\circ 9'$ and $154^\circ 34'$), BOB (90° and $125^\circ 9'$) and AOA ($79^\circ 38'$) shown in Fig. 4.A.1. The nearest

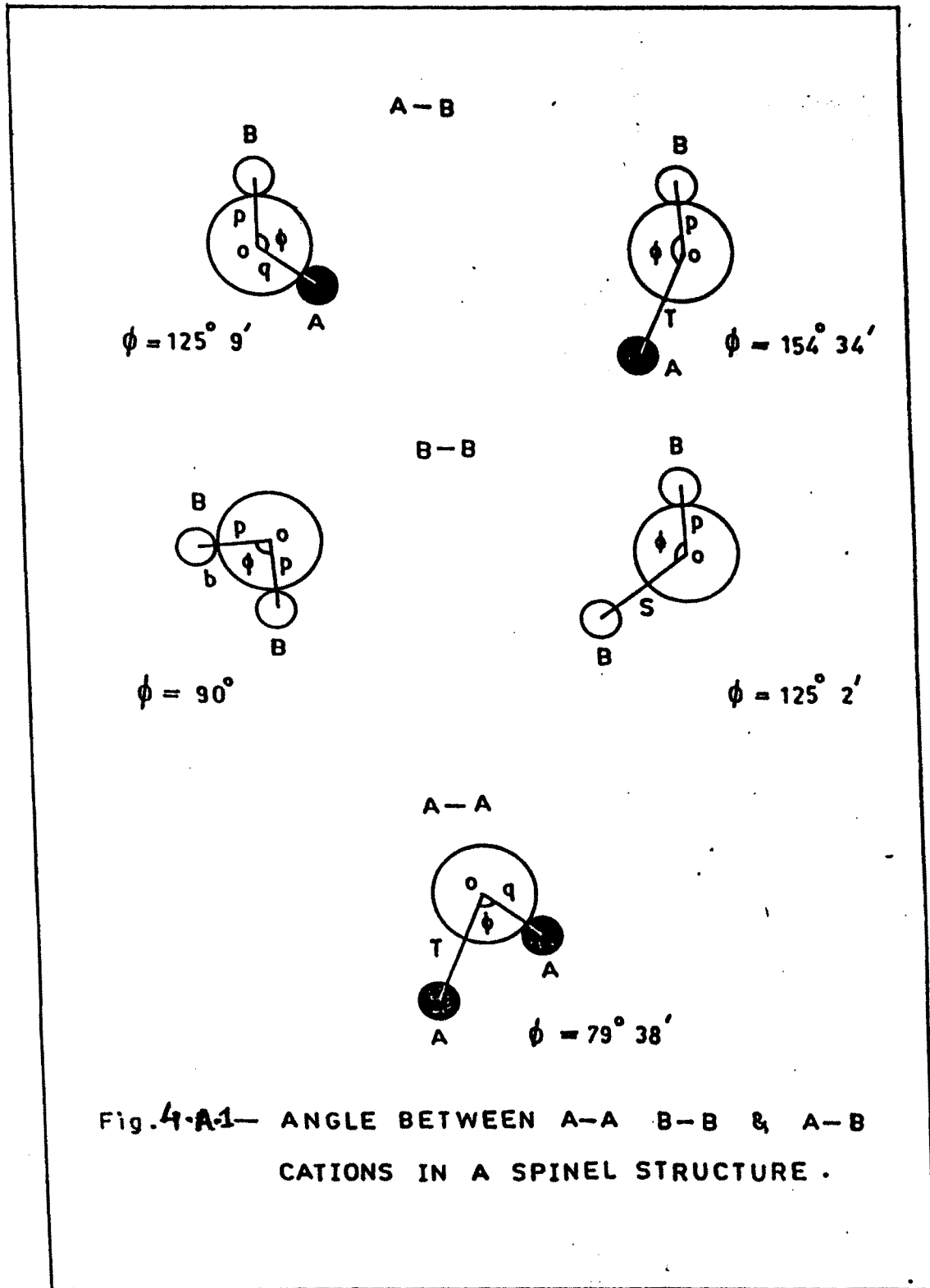


Fig. 4-A-1— ANGLE BETWEEN A-A B-B & A-B
CATIONS IN A SPINEL STRUCTURE .

to perfect alignment are Fe_A and Fe_B ions making an angle of $154^\circ 34'$, thus giving the strong antiferromagnetic coupling [11].

4.A.2 Magnetic Anisotropy

The term anisotropy is used to describe the directionality of magnetization along a certain crystallographic direction known as easy direction. The anisotropy energy is the energy required to change the direction of magnetization from easy to hard direction. It plays an important role in determining the properties such as permeability, hysteresis and magnetostriction (12). For cubic material anisotropy energy is given by

$$E_A = K_1[\alpha_1^2\alpha_2^2 + \alpha_2^2\alpha_3^2 + \alpha_3^2\alpha_1^2] + K_2[\alpha_1^2\alpha_2^2\alpha_3^2] \dots 1$$

where K_1 and K_2 are anisotropy constants depending upon temperature and material used. These constants determine the direction where E_A is minimum and α_1 , α_2 , α_3 are direction cosines. When magnetization vector deviates from preferred direction the anisotropy energy increases. The anisotropy constant varies with the crystal structure and kinds of magnetic ions involved. The electronic structure of magnetic ion also contributes to an anisotropy constant [13]. The magnetic anisotropy may also arise due to stress anisotropy and shape anisotropy.

The anisotropy constant K_1 for ferrite is found to vary from 10^4 erg/cm³ for cobalt ferrite to 10^{-5} erg/cm³ for Ni ferrite [14].

4.A.3 Magnetostriction

Ferrites exhibits magnetostriction wherein dimensional changes are associated with magnetization due to lowering of anisotropy energy by deformation of the crystal lattice.

When magnetic material is magnetized, its physical dimensions change. The phenomenon is known as magnetostriction and is related to thermal anomalies shown by ferrimagnetic substances around the Curie point.

The magnetostrictive energy is the magnetostriction parameter and is given by,

$$E = 3/2 \cdot \lambda_s \sigma$$

where, λ_s - saturation magnetization

σ - applied stress

Here, energy should be minimized to give the domain, freedom of motion.

For cubic material, the change in dimensions are isotropic i.e. only the volume changes takes place. But for hexaferrite change in volume and shape are observed. These changes occur even when the material is cubic but magnetic order is non-cubic. This is due to

the dependence of exchange energy on interatomic spacing. The magnetostriction is closely related to crystal anisotropy and direction of magnetization. The Nickel ferrite shows decrease in its length by 45ppm in the direction of magnetization.

4.A.4 Magnetization Process

A demagnetized ferrimagnetic material exhibits a state of zero magnetization. When sufficiently large magnetic field is applied to a ferro or ferrimagnetic substance, the magnetization changes from zero to saturation value. This was explained first by Weiss [15] on the basis of his domain theory. The building blocks of this theory are the domain and domain walls. These domains are arranged such that, the net magnetization is zero. The existence is consequence of process which minimize the free energy of the system. The other independent variables describing the magnetic state are the direction of the magnetization within the domains and the positions of the domain wall. The magnetization is constrained to be homogeneous inside the domain and its direction to vary within the domain wall.

The magnetization process takes place and a ferro or ferrimagnetic substance become magnetized due to domain boundary displacement and domain rotation. Both

processes can take place irreversibly resulting in a hysteresis loop. Domain rotation are mostly associated with intrinsic properties viz. the chemical composition of the material. Domain boundary displacement depends not only on the intrinsic properties but also on factors concerned with the sintering process such as porosity, size and shape of pores, and shape of crystal.

The process of magnetization of the specimen to saturation involves its conversion to a single domain state so that the magnetization vector lies parallel to applied field. According to domain theory, this can happen in two ways.

1. Domain that are oriented with respect to the applied magnetic field may grow at the expense of the other domain that are unfavourably oriented. On reversing the field, however, the domain boundaries return to their original position. This process of magnetization is called reversible boundary displacement.

2. The magnetization vector within each domain may rotate in the direction of field when the applied field is large. This process is called as magnetization by domain rotation. Here spin have to be turned from an easy direction to hard direction. The rotation of domains have been observed by Berkhausen [16]. He has

shown that, the discontinuous variation of the magnetization at low field takes place where the field is continuously increasing. These are known as Barkhausen jumps. Magnetization by domain rotation requires large energy.

4.A.5 Shape of hysteresis loop and domain state

Hysteresis study on ferrites gives a valuable data on permeability, saturation magnetization, coercive force and remanance ratio which are helpful to decide the nature of application of ferrites.

Hysteresis properties are mainly dependent on chemical composition, crystal structure, cation distribution, heat treatment, sintering atmosphere and final fabrication. The experimental technique for the measurement of magnetic properties are described by Maxwell [17].

The variation of magnetization with magnetic field usually depends upon nature of material but the curves have a general shape shown in Fig. 4.A.2. At the beginning the material is in the demagnetization state as shown at point 'O'. On the application of magnetic field, the magnetization increases until the saturation value is reached, the behaviour shown by curve OABC. This part of the curve is called magnetization curve. By carrying out the operation of reducing the magnetic

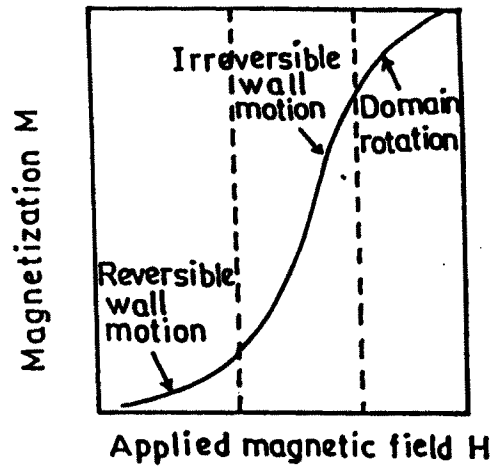


Fig. 4·A·1(a) — A TYPICAL MAGNETIZATION CURVE.

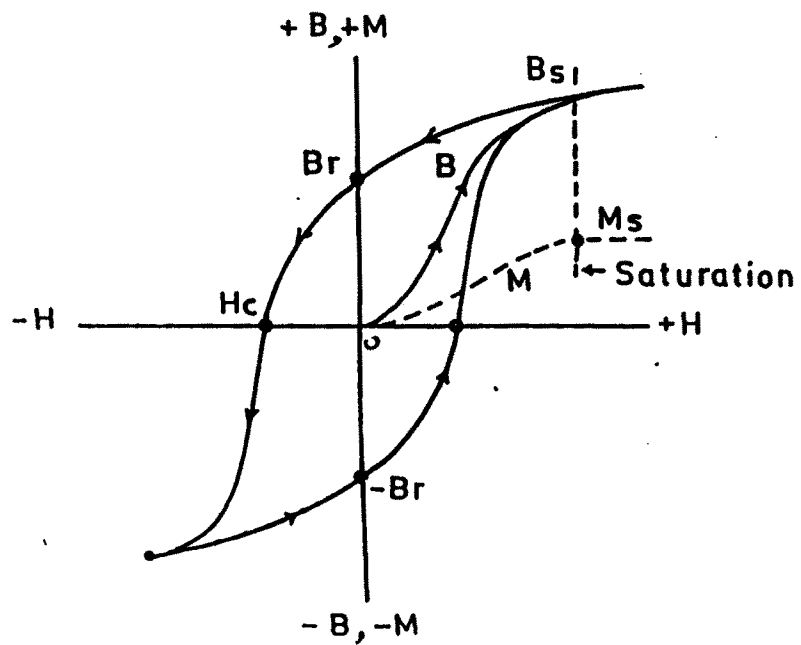


Fig. 4·A·1(b) — GENERAL FEATURES OF HYSTERESIS LOOP.

field to zero, increasing it in the reverse direction, decreasing it to zero and then increasing it to the original value, the curve CDEFGC results. This curve is known as hysteresis curve or hysteresis loop and is symmetric in nature.

The hysteresis loops of micro-powders can be classified in four types [18] namely,

- 1) Multi-domain (MD)
- 2) Superparamagnetic (SP)
- 3) Single-domain (SD-VA)
- 4) Single-domain (SD-CA)

In the initial part of hysteresis curve, reversible wall displacement takes place. Berkhausen jump and irreversible wall displacement predominate in the central part of the curve. On reducing the field, the domains relax to the nearest easy direction of magnetization because of anisotropy forces. On reversing the field, some boundary movements followed by Berkhausen jump takes place. Towards the bottom of the curve, rotation predominate again the saturation in the reverse direction is reached.

Silent features of the research work carried out in the field are -

1. Loop shapes are independent of the parameters of the intensity of magnetization and magnetocrystalline anisotropy constant (K_1).

2. Single domain (SD) and superparamagnetic (SP) shapes are temperature dependent where as multidomain (MD) shapes are temperature independent.

3. Experimentally determined shapes agrees with theoretically observed shapes for SD and SP cases while for MD cases it is not so.

4.A.6 Experimental Techniques

The experimental set up is shown in Fig. 4.A.3. The essential parts of the hysteresis loop tracer [19] are

1. Electromagnet
2. Pickup coil system
3. Balancing and integrating network
4. Preamplifier

1. Electromagnet

The two C cores (English electric Co-type WR/110/32/13) of laminated grain oriented silicon steel with cross-section of the holes $5 \times 2.5 \text{ cm}^2$ have been used for this purpose. From one of C-cores a piece of 1.2 cm in thickness was cut out to get a pole gap of 1.2 cm. The two C-cores were joined together. the energizing coil for the magnet consist of 2200 turns of 20 swg super enamelled copper wire (resistance 11.5

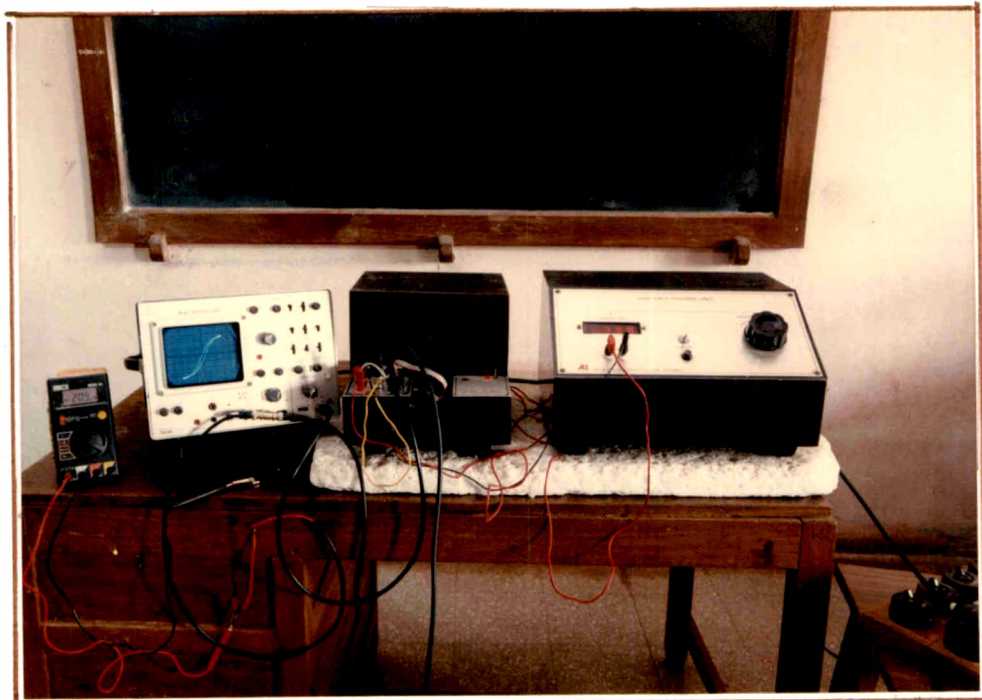


FIG.4.A.3. EXPERIMENTAL SET UP FOR HYSTERESIS LOOP TRACER

ohms) wound on a perspex former and held together on the wooden base.

2. Pick-up coil system

A multicoil which can be introduced in the pole gap serves as a pick up coil system. It consists of different windings; one over the other wound with 39 swg super enamelled copper wire on a perspex former. A multicoil is connected to the balancing and integrating network to a amplifier and then to the Y-plates of the oscilloscope. The input of the X-plate is taken from the emf developed across a resistance connected in series with proper inductance and variable resistance is also provided. The multiple unit was slid into the pole gap and current in the energizing coil was increased to produce the required field. The potentiometer and variable resistance in the balancing network were adjusted to get a horizontal trace on the oscilloscope. After reducing the current to zero, the multicoil was pulled out and the ferrite pellet kept at the central gap in the multicoil spool and next introduce into the pole gap. The current in the energizing coil was raised to a sufficient value till the sample saturates. The hysteresis loop produced on the oscilloscope was recorded for an accurate measurement of magnetization.

Pure Nickel (99.9%) in the form of cylindrical pellet ($M_s=55.35$ emu/gm at 27°C) was used for the calibration of Y-axis. The horizontal scale was calibrated by measuring the magnetic field. With a sensitive gaussmeter while d.c. was passed through the energizing coil. For obtaining hysteresis loop a.c. field are used and hence the necessary corrections for d.c. fields were incorporated.

4.A.7. Calculation of M_s and n_e

The vertical displacement on oscilloscope and corresponding reading in mv were taken for Ni sample of mass 0.267 gms. As the standard magnetization for Ni sample is 53.35 emu/gm and applied field is 3K gauss.

The total magnetization of Ni sample is,

$$53.35 \times 0.2679 = 14.289 \text{ emu}$$

The vertical divisions on C.R.O. is 22 and hence the calibration factor is,

$$\text{C.F.} = \frac{\text{Total magnetization of Ni sample}}{\text{Reading for Ni-sample}}$$

$$\begin{aligned} \text{C.F.} &= \frac{14.289}{22} \\ &= 0.6496 \text{ emu/div} \end{aligned}$$

The vertical reading for the samples were taken at room temperature. By using these readings of magnetization of samples were calculated

$\sigma_s = \text{Reading of pellet} \times \text{C.F.}$

The σ_s is emu/gm.

$$\sigma_s' = \frac{\sigma_s}{\text{mass of pellet}}$$

and M_s is calculated as,

$$M_s = (1-p) d_x \cdot \sigma_s'$$

where, porosity = $p = d_x - d_a/d_x$

$$d_x = \text{X-ray density} = \frac{2 \times \text{mol. wt. (sample)}}{N a^3}$$

where, $N = \text{Avogadro's Number}$

$a = \text{lattice constant}$

$$\begin{aligned} d_a = \text{physical density} &= \frac{\text{mass of pellet}}{\text{volume of the pellet}} \\ &= \frac{m}{\pi r^2 t} \end{aligned}$$

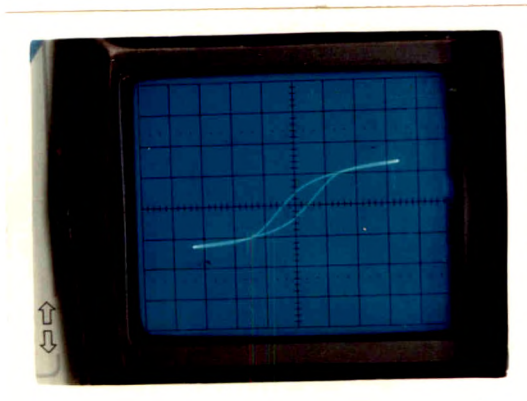
The magnetic moment per formula unit in Bohr magnetons (n_B) is given by

$$n_B = \frac{\text{mol. wt.} \cdot \sigma_s'}{5585}$$

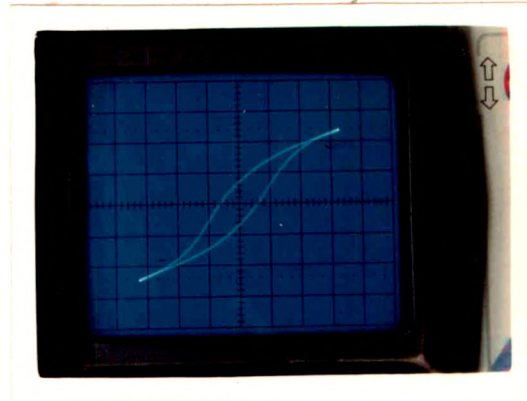
hence from above formula, M_s and n_B were calculated.

4.A.8 Results and discussion

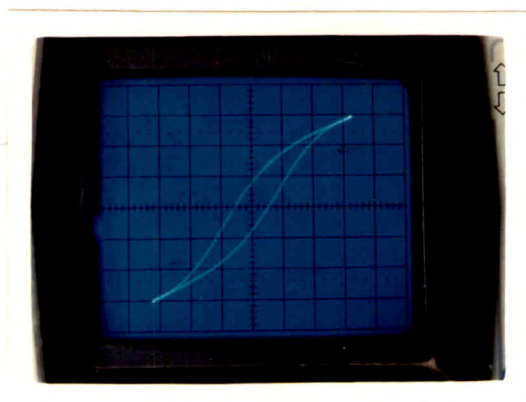
Hysteresis loops for samples of Ni ferrite in the series $\text{NiAl}_x\text{Fe}_{2-x}\text{O}_4$ are shown in Fig.4.A.4. From the hysteresis data the values of saturation magnetization



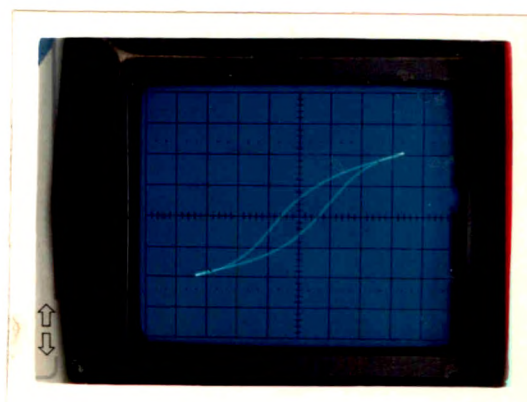
Ni-Sample



X=0.0

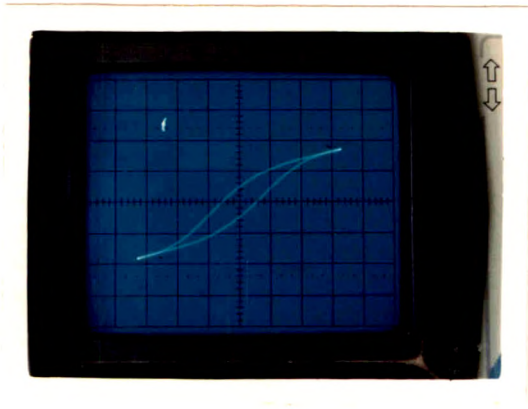


X=0.2

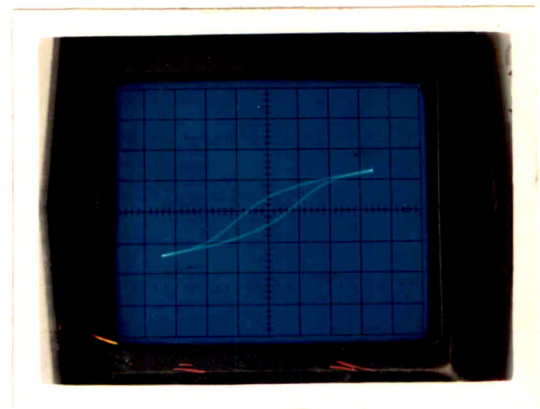


X=0.4

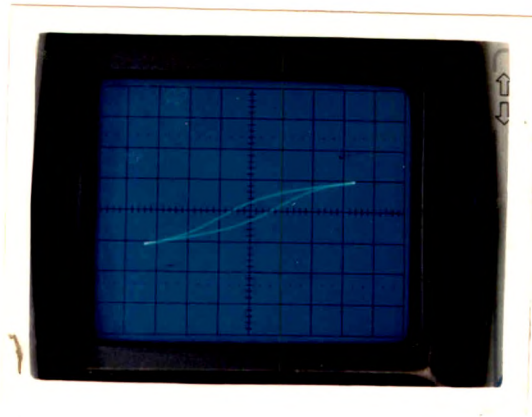
FIG.4.A.4. HYSTERESIS LOOPS FOR $\text{Ni Al}_x \text{Fe}_{2-x} \text{O}_4$.



$x=0.6$



$x=0.8$



$x=1.0$

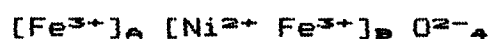
FIG.4.A.4. HYSTERESIS LOOPS FOR $\text{NiAl}_{x/2-x/4}\text{O}_4$.

(Ms) and magnetic moment (n_B) were calculated at room temperature and are noted in Table 4.A.1.

From this Table, it can be seen that, saturation magnetization and the magnetic moment decrease with increasing Al content [Fig.4.A.5]. This variation can be explained in terms of cation distribution and Al^{3+} content.

In the present system, the values of magnetic moment of $NiFe_2O_4$ is slightly lower than the value of magnetic moment that has been reported earlier [20,21,22]. This could be due to changes in sintering conditions.

Magnetization in ferrites results from the distribution and alignment of magnetic ions on the tetrahedral and octahedral cation sites. Nickel ferrite cooled slowly from sintering temperature has a structure of a completely inverse spinel. For Nickel ferrite the cation distribution is expressed as,



The standard magnetic moment for Ni^{2+} is $2.2 \mu_B$ and for Fe^{2+} is $5 \mu_B$ [20]. The Fe^{3+} ions on A-site are coupled with their spins antiparallel to the Fe^{3+} ions on B-site, so that, the net magnetic moment is due to Ni^{2+} metallic ions. This shows why the magnetic moment is a function of Ni content.

TABLE - 4.A.1.

Saturation magnetization(M_s), $4\pi m_s$ and Magnetic moment (n_B)
of $NiAl_xFe_{2-x}O_4$

| X | Saturation Magnetization M_s emu/cc | $4\pi m_s$ | Magnetic moment ' n_B ' |
|------|---|------------|------------------------------|
| 0.00 | 127.699 | 1604.707 | 1.5217 |
| 0.20 | 117.304 | 1474.086 | 1.4208 |
| 0.40 | 73.226 | 920.185 | 0.9611 |
| 0.60 | 54.556 | 685.574 | 0.7278 |
| 0.80 | 54.659 | 686.860 | 0.6883 |
| 1.00 | 45.774 | 575.214 | 0.5351 |

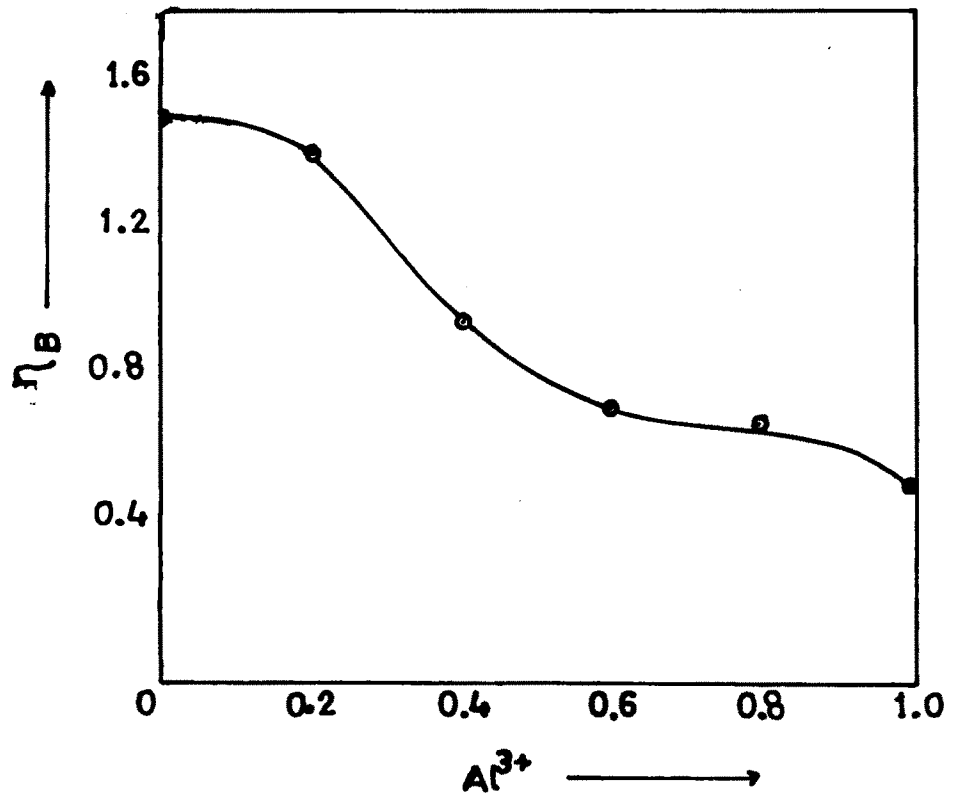


Fig.4.A5. Variation of magnetic moment with Al^{3+} content

Many investigators have studied the magnetic properties of Ni ferrites and Ni containing ferrites [20,22,23,24,25]. Krishnan [25] has studied the magnetic properties of NiFe_2O_4 and has concluded that this ferrite if cooled rapidly, from higher temperature, a certain amount of Ni^{2+} ions are frozen in the A-site which cause a small change in the magnetic moment.

The decrease in saturation magnetization with increasing Al^{3+} content can be explained on the basis of changes in the magnetization M_A and M_B of tetrahedral and octahedral sublattices respectively. Al^{3+} ions besides preferring B-sites, have also a small tendency to occupy the A-site, the partial replacement of Fe^{3+} ions each having a magnetic moment of $5\mu_B$ by diamagnetic Al^{3+} ions results in lowering the value of both M_A and M_B . The decrease in M_B , however, predominates over the decrease in M_A , thereby decreasing the net magnetization and hence n_B . Similar results were also observed in the case of Ni-Sn ferrites when Al^{3+} is substituted [26].

SECTION - B

A.C. SUSCEPTIBILITY

4.B.1. Introduction

The susceptibility is defined as the ratio of the magnetization (M) produced in the substance to the applied magnetic field (H).

$$\text{i.e. } X = M/H \text{ emu/cm}^3 \text{ Oe} \quad \dots \quad 4.B.1$$

A.C. susceptibility and magnetization studies explore the existence of multi-domain (MD), single domain (SD) and superparamagnetic (SP) particles in the materials [Fig. 4.B.1]. The demagnetized state of a ferro or ferrimagnetic body is normally presumed to be due to its subdivision into Weiss domains with Bloch walls separating them [27]. Grains having domain walls within them are called multidomain. If the grains cannot contain walls then they are called single domain. The studies of thermal variation of a.c. susceptibility explore the possibilities of existence of domains present in the material. Using this technique many workers [28,29,30] have investigated nature of magnetic domains in ferrites. The shapes of X_{ac} against T curves have been correlated with domain structure by Radhakrishnanmurthy [27].

In $X_{ac} - T$ curves, the Curie temperature has been estimated at a point at which the curve drops to zero.

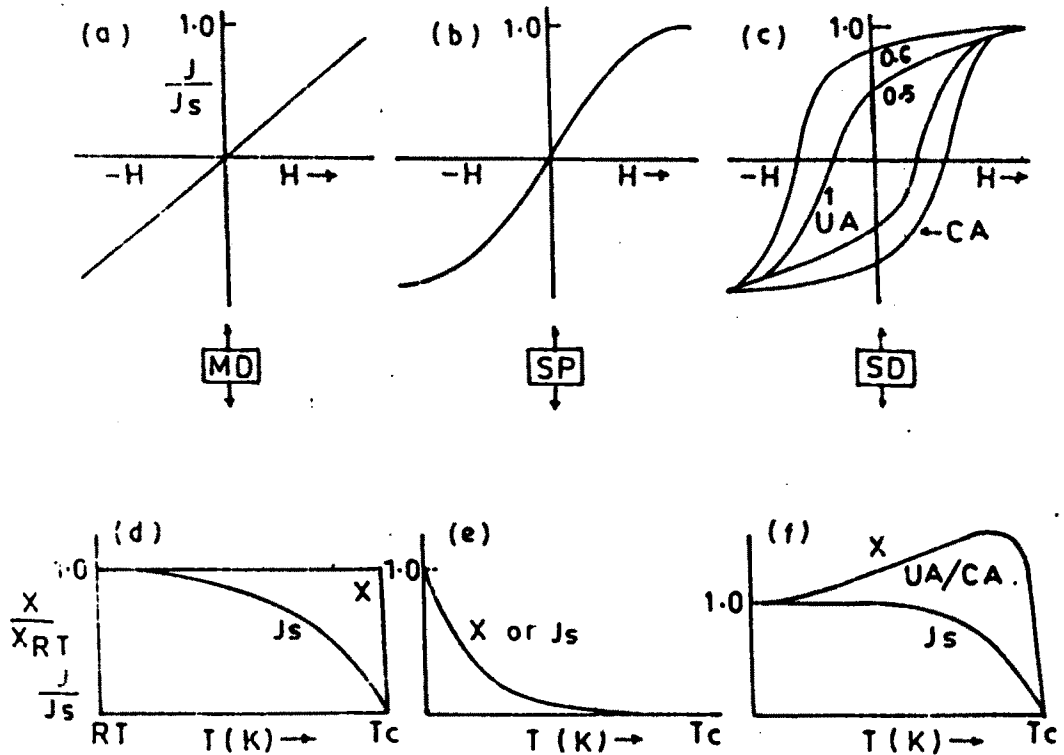


Fig. 4-B-1 Schematic hysteresis loops normalized $x-T$ and J_s-T curves for samples containing grains in different domain states, MD-multidomain SP-superparamagnetic and SD-optimum single-domain states. In (c) UA denotes dominant uniaxial anisotropy and CA dominant crystalline anisotropy. Interesting point to be noted is that the $x-T$ and J_s-T curves may be similar for a sample consisting of sufficiently fine SP particles.

The susceptibility study is very useful in order to invoke the grain size effects like a very fine stable simple domain (SD) particles becoming superparamagnetic (SP) particles on heating to temperature of several degrees below Curie temperature. The magnetic grains which have a few hundred Angstroms dimension are termed as single domain (SD) for which magnetization direction is fixed in space. The very small grains, upto about hundred Angstroms are called as superparamagnetic (SP). When thermal energy of SD particles becomes comparable to effective magnetic anisotropy energy, magnetization direction fluctuates between the easy axes of the grains. In such a state the grain is said to be exhibiting superparamagnetic (SP).

For volume V of the grains, the temperature is referred to as the blocking temperature (T_b) which is less than the Curie point (T_c). The volume V , saturation magnetization (M_s) and coercive field (H_c) are related by the relation given Neel [31] as,

$$V M_s H_c = 2K T_b \quad \dots \quad 4.B.2.$$

where K - Boltzmann constant

Thus superparamagnetic can be changed to single domain by cooling the ferrites below their T_b . The susceptibility becomes infinite and the spontaneous

magnetization appears at a particular temperature called as Curie or Neel temperature.

The transition from ferro to para region is not sharp in each case but gives tailing effect due to spin clusters (i.e short range spin ordering). The low field a.c. susceptibility plays an important role in the study of spin glass behaviour. The spin glass behaviour is characterized by the cusps at low temperature [32,33]. Sudden change in X_{ac} -T curves as well as values of X_{ac} [34,18] have been observed. Bean [18] has stated that for MD particles, very small values H_c and M_r/M_s are observed where as for SD particles these values are larger.

High temperature a.c. susceptibility measurement were first carried out by Hopkinson [36] on iron. He has observed a peak just before T_c . Domain structure in ferrites have been studied by number of workers [37,38]. Three types of peaks have been reported in X_{ac} -T curves -

1. Hopkinson peak is the one occurring just before T_c of any magnetic material in the MD state.

2. Isotropic peak which could be seen clearly for a magnetic material in M.D. form and only if the material has a temperature at which the magnetocrystalline anisotropy is zero.

3. SD peak which could be obtained only if the sample under investigation has a substantial proportion of SD particles in it and occurs at blocking temperature.

4.B.2 Experimental Techniques

The experimental set up of a.c. susceptibility is shown in Fig.4.B.2. The low field a.c. susceptibility measurement of powdered samples were taken in temperature region 300-850 °K using the apparatus developed by Likhite et al. [39].

The experimental set up consists of two Helmholtz coils to produce uniform field at the pick up coil. A furnace fabricated by winding the platinum wire on silica tube is used to heat the sample. To avoid overheating of the coils a glass jacket with water circulations is used. The furnace is inserted in glass-jacket which is placed in the center of pick up coil. Height of the sample tube is maintained in such a way that, the sample can stay at center of double coil. The current to the Helmholtz coil is supplied by an oscillator and a high quality power amplifier. The signal induced in the double coil, which is proportional to the rate of change of magnetic moment of the sample, is amplified, rectified and read out on digital voltmeter. The meter reading can be calibrated

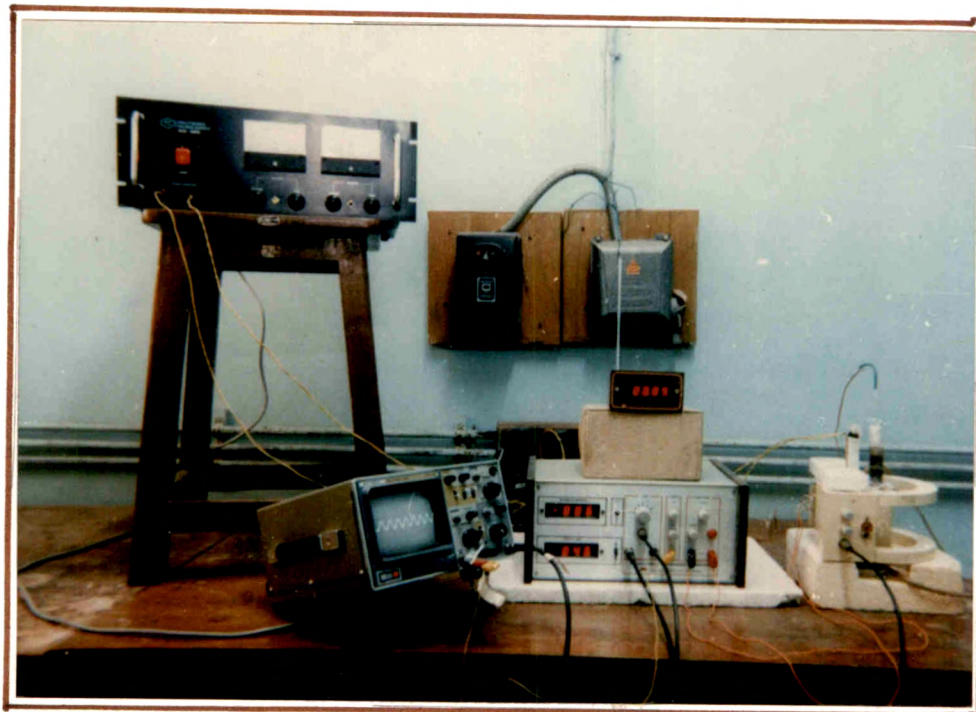


FIG. 4.B.2. EXPERIMENTAL SET UP FOR A.C. SUSCEPTIBILITY MEASUREMENT

in terms of magnetic moments. The temperature of the furnace is maintained by control over to power supply. The temperature was measured by calibrated platinum-rhodium thermocouple. The sample was gradually heated and at various temperatures the signal corresponding to the magnetic moment was recorded. The heating was continued till the signal was reduced to zero.

4.B.3 Results and discussion

The variation of normalized a.c. susceptibility (X_T/X_{RT}) as a function of temperature for the samples $NiAl_xFe_{2-x}O_4$ with $x=0, 0.2, 0.4, 0.6, 0.8$ and 1.0 is shown in Fig. 4.B.3. A peak at blocking temperature (T_b) is exhibited by almost every sample in the series. It suggests that below the blocking temperature (T_b) the samples are in a single domain (SD) + multidomain state (MD) and above blocking temperature they are in superparamagnetic (SP) state.

From the variation of normalized a.c. susceptibility (X_T/X_{RT}) with temperature it can be observed that,

- 1) All the samples exhibit a peak at blocking temperature (T_b) and then the susceptibility drops suddenly near Curie temperature.
- 2) The samples with $x = 0$ and 0.2 contain SD particles which is supported by the observation of

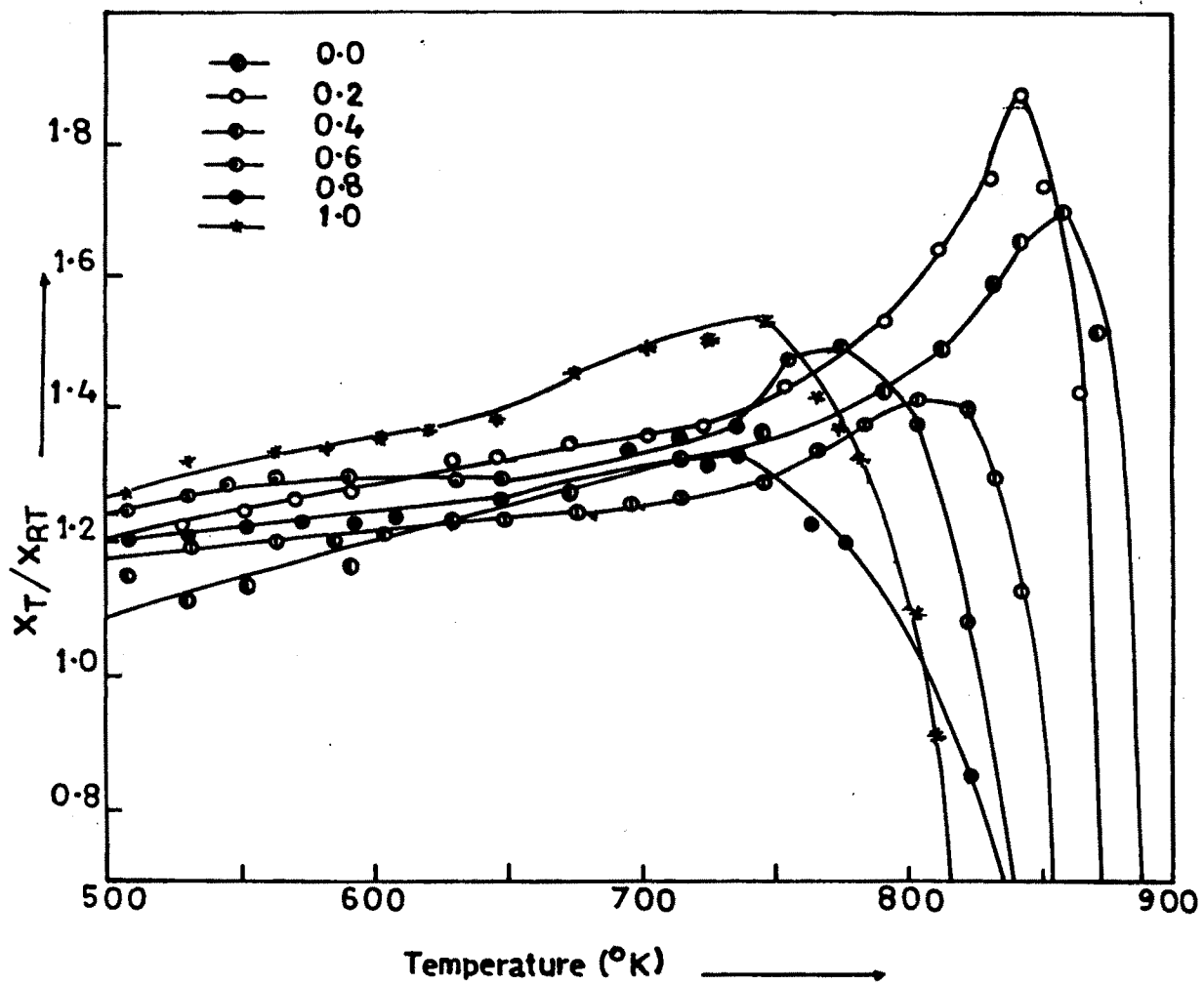


Fig.4B.3. Variation of normalised A.C. susceptibility with temperature for $\text{NiAl}_x\text{Fe}_{2-x}\text{O}_4$.

higher values of H_c . For these samples, the curve drops sharply after blocking temperature (T_b).

3) For $x = 0.4$ to 0.1 , the addition of Al^{3+} ions to the system, the drop is slow. This is due to the existence of multidomain + single domain particles in ferrite.

4) For all the samples, peak height goes on decreasing on addition of Al^{3+} ions.

5) All the samples show a sharp decrease in normalized a.c. susceptibility (X_T/X_{RT}) with temperature near Curie temperature (T_c) which indicates that, impurity phases are not present in the sample and there is single phase formation. The fact is evidenced by XRD analysis of our samples (Chap. II). Also cubic structure of the sample contain single domain + multidomain type of particles [40].

For single domain (SD) particles, the coercive force (H_c) is large, whereas it leads to zero for superparamagnetic (SP) particles [18]. The susceptibility which is inversely proportional to H_c , is large for superparamagnetic S(P) particles of the same material and hence there is peak in normalized a.c. susceptibility (X_T/X_{RT}) and temperature at blocking temperature (T_b).

It is interesting to note that, Curie temperature (T_c) decreases as the content of Al increases. This is

TABLE - 4.B.1.

Curie temperature data

| X | Curie Temperature 'Tc' (°C) | |
|-----|-----------------------------|---------------------|
| | D.C. Conductivity | A.C. Susceptibility |
| 0.0 | - | 585 |
| 0.2 | 571 | 574 |
| 0.4 | 556 | 552 |
| 0.6 | 549 | 546 |
| 0.8 | 525 | 526 |
| 1.0 | 515 | 510 |

due to the removal of magnetic ions (Fe^{3+}) from magnetic sublattice and substitution of non-magnetic ion Al^{3+} in its place. This weakens the net superexchange interaction. Similar decrease in T_c is observed when trivalent Al and Ga is substituted for Fe^{3+} and in Ni ferrite [41], Li ferrite [42] and Ni-Sn ferrite.

The data on Curie temperatures obtained [26] from d.c. conductivity and a.c. susceptibility measurement is given in Table 4.B.1. It is observed that Curie temperatures measured by these methods are nearly the same.

References

1. Stern E.
Microwave materials and applications
J. Applied Phys. 38, 3 (1967) 1397
2. Lee E.W. and Lynch A.C.
Adv. in Phys. (1959) 292
3. Hoh S.R.
"Evaluation of High performance core materials"
Tele - Tech. 2 (1953) 86
4. Richards E.E. and Lynch A.C.
Soft magnetic materials for telecommunications
Pergamon, Press Ltd. (1953)
5. Neel L.
Properties of magnetic ferrites!,
ferromagnetization and antiferromagnetism
Ann. Phys. 3 (1948) 137
6. Alper A.M.
"High temperature oxides"
Academic Press, N.Y. (1971)
7. Srivastav C.M., Patani M.J. and Shrinivasan T.T.
J. Appl. Phys. 53 (3) (1982) 2107
8. Snoek J.L.
Philips Tech. Rev. 8 (1946) 363
9. Gorter E.W.
Phillips Tech. Rev. 8 (1946) 295
10. Goodenough J.B.
'Magnetism and chemical bond'
Interscience, London (1962)
11. Gray T.J.
'Oxide Spinel In High Temperature Oxides'
Part-IV Ed. A.M. Alper, Academic Press, N.Y.
(1971) 77
12. Broese Van Groenou, Bangers P.F. and Stuijts A.L.
Mater. Sci. Eng. 3 (1968/69) 317
13. Kanamari J.
In 'Magnetism' G.T. Rado and Shull C.G. [edi].,
Academic Press N.Y. (1963) 127

14. Viswanthan B. and Murthy V.R.K.
'Ferrites Materials'
Narosa Publishing House, New Delhi (1990)
15. Weiss P.
J. De. Physique 6 (1907) 661
16. Barkhausen H.
Phys. Zeits, 20 (1919) 401
17. Maxwell S.P.
The Marconi Rev. (1st Quarter) (1970) 20
18. Bean C.P.
J. Appli. Phys. 26 (1955) 1381
19. Likhite S.D., Radhadrishnamurthy C. and
Sahasrabudhe P.W.
Ind. Acad. Sci. 87 (A) (1978) 245
20. Robertson J.M. and Poynton A.J.
Solid State Communications, 4 (1966) 257
21. Elwell D., Parker R. and Tinsley C.J.
Solid State Communication 4 (1966) 69
22. Petrov.V.V., Chukalkin Yu. G. & Goshchitskil B.N.
Sov. Phys. Solid State, 22 (1980) 2
23. Kiran H.V., Shashimohan A.L., Chakroborty D.K. and
Biswas A.B.
Phys. Stat. Solid; (a) 66 (1981) 743
24. Seshan K., Shshimohan A.L., Chakroborty D.K. and
Biswas A.B.
Phys. Stat. Solid (a) 68 (1981) 97
25. Krishnan R.
Phys. Stat. Solid 32 (1969) 695
26. Babbar V.K. and Chandel J.S.
Bull. Mat. Sci. 18, 8(1995) 997-1005
27. Murthy C.R.K.
J. Geogological Soc. Ind. 28, (1985) 640-651
28. Baldha G.D., Upadhyay R.V. and Kulkarni R.G.
Mat. Res. Bull. 21, (1986) 1051-1055
29. Patil B.L., Sawant S.R. and Patil S.A.
Czech. J. Phys. 43, 1 (1993) 87-93

30. Kulkarni R.G. and Upadhyay R.V.
Mat. Lett. 4, 3 (1986) 168-170
31. Loroia K.K. and Sinha A.P.B.
Ind. J. Pure and Appli. Phys. 1 (1963) 215
32. Wohlfarth E.P. (Ed).
"Ferromagnetic Materials" 2 (1980) 204
33. Chakravarthy R., Madhav Rao L, Paranjpe S.K. and
Kulshrestha S.K.
Proc. ICF 5, (1989) (India)
34. Upadhyay R.V.
Ind. J. Pure and Appli. Phys. 31 (1993) 333
35. Radhakrishnamurthy C., Likhite S.D. and Naterajan
J. Mag. and Mag. Mater. 15-18 (1980) 195
36. Hopkinson J.
Phillips Trans. Roy. Soc. (London) AL 80 (1989)
443
37. Venkatesh Rao and Keer H.V.
Pramana 19 (1982) 103
38. Stoner E.C. and Wolhfarth E.P.
Philips Trans. Roy. Soc. A-240 (1948) 599
39. Radhakrishnamurthy C., Likhite S.D. and
Shastri N.P.
Phil. Mag. 23. (1971) 603
40. Patil S.H.
Ph.D. Thesis, Shivaji University, Kolhapur (1993)
41. Louis R.Maxwell and Stanley J. Pickart
Physical Review 92 ,5 (1953)
42. Dionne G.F.
J. Appl. Phys. 40 (1969) 431